Am J Physiol Heart Circ Physiol 292: H3136–H3147, 2007.
First published March 2, 2007; doi:10.1152/ajpheart.00683.2006.

Dual cardiac contractile effects of the α_2-AMPK deletion in low-flow ischemia and reperfusion

Karla Carvajal,[1] Elham Zarrinpashneh,[2] Ondrej Szarszoi,[1] Frederic Joubert,[1] Yoni Athea,[1] Philippe Mateo,[1] Brigitte Gillet,[3] Sophie Vaulont,[4] Benoit Viollet,[4] Xavier Bigard,[5] Luc Bertrand,[2] Renée Ventura-Clapier,[1] and Jacqueline A. Hoerter[1]

[1]*INSERM U769, Faculté de Pharmacie, Université Paris-Sud, Châtenay-Malabry, France;* [2]*Division of Cardiology, School of Medecine, Université Catholique de Louvain, Brussels, Belgium;* [3]*RMN Biologique, Institut de Chimie des Substances Naturelles, Centre National de la Recherche Scientifique, Gif sur Yvette, France; and* [4]*Institut Cochin, INSERM U567, Centre National de la Recherche Scientifique UMR-8104, Université Paris 5, Paris, France; and* [5]*Département des Facteurs Humains, Centre Recherche Service Santé Armée, La Tronche, France*

Submitted 28 June 2006; accepted in final form 8 February 2007

Carvajal K, Zarrinpashneh E, Szarszoi O, Joubert F, Athea Y, Mateo P, Gillet B, Vaulont S, Viollet B, Bigard X, Bertrand L, Ventura-Clapier R, Hoerter JA. Dual cardiac contractile effects of the α_2-AMPK deletion in low-flow ischemia and reperfusion. *Am J Physiol Heart Circ Physiol* 292: H3136–H3147, 2007. First published March 2, 2007; doi:10.1152/ajpheart.00683.2006.—Because the question "is AMP-activated protein kinase (AMPK) α_2-isoform a friend or a foe in the protection of the myocardium against ischemia-reperfusion injury?" is still in debate, we studied the functional consequence of its deletion on the contractility, the energetics, and the respiration of the isolated perfused heart and characterized the response to low-flow ischemia and reperfusion with glucose and pyruvate as substrates. α_2-AMPK deletion did not affect basal contractility, respiration, and high-energy phosphate contents but induced a twofold reduction in glycogen content and a threefold reduction in glucose uptake. Low-flow ischemia increased AMPK phosphorylation and stimulated glucose uptake and phosphorylation in both α_2-knockout (α_2-KO) and wild-type (WT) groups. The high sensitivity of α_2-KO to the development of ischemic contracture was attributed to the constitutive impairment in glucose transport and glycogen content and not to a perturbation of the energy transfer by creatine kinase (CK). The functional coupling of MM-CK to myofibrillar ATPase and the CK fluxes were indeed similar in α_2-KO and WT. Low-flow ischemia impaired CK flux by 50% in both strains, showing that α_2-AMPK does not control CK activity. Despite the higher sensitivity to contracture, the postischemic contractility recovered to similar levels in both α_2-KO and WT in the absence of fatty acids. In their presence, α_2-AMPK deletion also accelerated the contracture but delayed postischemic contractile recovery. In conclusion, α_2-AMPK is required for a normal glucose uptake and glycogen content, which protects the heart from the development of the ischemic contracture, but not for contractile recovery in the absence of fatty acids.

glucose uptake; pyruvate; fatty acids; energetics; rigor; creatine kinase; ^{31}P-NMR spectroscopy; energetic cost of contractility

A MAJOR ENERGETIC sensor in the mammalian cell and regulator of cardiac metabolism is AMP-activated protein kinase (AMPK). AMPK activation switches on the ATP synthesis pathways and inhibits the ATP consuming pathways (for recent reviews, see Refs. 15, 52). Despite numerous investigations, and as stated previously (15), the question of whether AMPK activation is an ally or an enemy in the protection against ischemic damage is still controversial. On one side, AMPK activation may be beneficial because of increased ATP production by stimulation of glucose uptake, glycogenolysis, and glycolysis, as well as fatty acid oxidation (15); as a result, a chronic decrease in AMPK activity could be expected to induce energy deficiency and to impair cardiac contractile function during an ischemia-reperfusion challenge. However, AMPK activation may contribute to postischemic mechanical deficiency and reperfusion injury from stimulation of fatty acid oxidation, which inhibits glucose oxidation (40). In this sense, AMPK deficiency could be predicted to attenuate myocardial damage of the postischemic heart.

The model of knockout of the α_2-catalytic unit (α_2-KO), the main cardiac α-isoform (50), results in complete abolition of cardiac α_2 activity without compensation by α_1-isoform. In this mouse model, α_2 deletion accelerated the development of the ischemic contracture in global ischemia but did not alter the postischemic contractile recovery (53). An early rise in the ischemic contracture has already been observed in other transgenic models: the overexpression of dominant-negative α_2 kinase model (51) and the α_2 kinase dead (KD) model (39). However, a major difference compared with a recent study from our group (53) showing preserved contractile recovery after global ischemia with glucose and pyruvate as substrates is the increased apoptosis and poor postischemic recovery of the KD mutant after low-flow ischemia (LFI) in the presence of fatty acids, which lead the authors to conclude that the activation of α_2-AMPK plays an important protective role in limiting the damage of ischemia-reperfusion episodes (39). However, because KD mutants have decreased activity of both α_2- and α_1-AMPK isoforms compared with the α_2-KO, it is not yet clear whether the protective role of AMPK is model and/or isoform dependent.

Our aim was to characterize the consequences of α_2-AMPK deletion on the basal and ischemic heart function using the LFI model, which better simulates the conditions prevailing in an infracted region than global ischemia: indeed, during an acute occlusion of the left anterior descending coronary artery, the collateral flow in the infarct zone still represents 10–40% of the baseline flow (11). We investigated some of the mechanisms of the glycolytic pathway involved in the response to an

Address for reprint requests and other correspondence: J. A. Hoerter, INSERM U-769, Faculté de Pharmacie, 5 rue Jean Baptiste Clément, F-92296 Châtenay-Malabry, France (e-mail: jacqueline.hoerter-buraud@u-psud.fr).

The costs of publication of this article were defrayed in part by the payment of page charges. The article must therefore be hereby marked "*advertisement*" in accordance with 18 U.S.C. Section 1734 solely to indicate this fact.

 0363-6135/07 $8.00 Copyright © 2007 the American Physiological Society

Downloaded from journals.physiology.org/journal/ajpheart at Univ Catholique Louvain Bruxe (130.104.166.176) on August 18, 2020.

ischemia-reperfusion insult. We addressed specifically the role of the α_2-AMPK in the glycolytic pathway in the absence of fatty acids because their presence was shown to exacerbate the consequences of the ischemia-reperfusion insult in the KD model (39). The addition of insulin to the perfusate would have represented a more "physiological" medium; however, we deliberately chose a simple protocol to avoid the complex interference between insulin and both the metabolic responses to ischemia and AMPK activation (12, 16, 27). Pyruvate was used as substrate because its oxidation is efficient in LFI (33). Moreover, as an antioxidant, pyruvate allows us to study the role of α_2-AMPK in conditions while minimizing the complex and not fully understood interferences of oxygen and nitrosyl radicals with AMPK activity. We assessed the consequences of α_2 deletion on the contractility, oxygen consumption ($\dot{V}O_2$), glucose transport, and energetics in basal normoxic conditions and during an LFI and reperfusion episode. We also assessed whether the protective role of AMPK observed in the presence of fatty acids in the KD mutant was also present in the α_2-KO mouse heart.

METHODS

Animals. Nine-month-old male α_2-KO (−/−) and wild-type (WT; +/+) mice were obtained by crossing heterozygote α_2-AMPK (−/+) (50). The genotype of the offspring was checked by PCR on DNA extracted from the tail. The animals were fed ad libitum a standard chow except for the estimation of glucose transport and phosphorylation in which the animals were fasted for 12–18 h. The investigation was conducted in accordance with our institutional guidelines defined by the European Community guiding principles in the care and use of animals and French decree no. 87/848 of October 19, 1987. Authorizations to perform animal experiments according to this decree were obtained from the French Ministry of Agriculture, Fisheries, and Food (no. 7475, May 27, 1997).

Perfused heart. Mice were anesthetized by intraperitoneal injection of urethane (2 mg/g). The heart dissection was performed in a solution containing low calcium (0.4 mM) and high glucose (15 mM). The perfusion solution contained (in mM) 143 sodium, 6 potassium, 1.8 calcium, 1 magnesium, 1.1 mannitol, 20 HEPES, 11 glucose, and 2 pyruvate and was oxygenated with 100% O_2. pH was adjusted to 7.35 at 36.5°C. Langendorff retrograde perfusion of the hearts was performed at a constant flow of 2.5 ml/min (the average flow value measured in the same hearts perfused at a constant pressure) (53). A subset of five WT and five α_2-KO hearts was perfused for 15 min with a solution containing 0.4 mM oleate, 1% BSA (dialyzed at 4°C overnight), and 5 mM glucose. These hearts were then submitted to LFI and reperfusion (see below). To ensure adequate oxygenation and thermoregulation, the silicon perfusion line was surrounded by circulating water continuously bubbled with 100% O_2 at 36.5°C down to the heart. A latex balloon inserted in the left ventricle chamber was inflated to maximal isovolumic condition of work [end-diastolic pressure (EDP) of 8–10 mmHg]. The on-line measured parameters included heart rate (in beats/min), left ventricle systolic developed pressure (LVDP), EDP, and coronary pressure (all pressure expressed in mmHg). Contractility was estimated as the rate-pressure product (RPP; expressed in 10^4 mmHg·beats·min^{-1}). Hearts were freeze clamped to measure their ATP, phosphocreatine (PCr), and glycogen contents (in nmol/mg protein) and to assess the state of AMPK phosphorylation at the end of control, LFI, and reperfusion periods.

NMR spectroscopy. ^{31}P NMR spectra were acquired on an Inova Varian at 9.4-T wide-bore magnet in 10-mm-diameter tubes using an 80° pulse angle, 4,000 data point acquisition, a spectral width of 10,000 Hz, an acquisition time of 0.205 s, a repetition time of 2 s, 32 scans, zero filling to 8,000, and line broadening of 30 Hz. After 10 min of equilibration, four partially saturated spectra and a fully relaxed spectrum (repetition time 10 s) were acquired. Stability of the preparation was checked by comparing control spectra acquired before and after the magnetization transfer experiment: any heart showing >10% variation in its metabolite content was discarded. In a pilot study, we found the kinetics of depletion of PCr during global normothermic ischemia to be too fast for accurate detection and PCr content too low to allow the determination of creatine kinase (CK) flux. WT and α_2-KO hearts, freeze clamped in control, showed similar ATP contents measured by spectrofluorometry; the average ATP content (19.0 ± 0.5 nmol/mg protein, $n = 10$) was used as a reference for the NMR quantification of PCr, P_i, and 2-deoxy-D-glucose-6-phosphate (2DG6P) concentrations after correction for incomplete magnetic relaxation as described previously (22). A cytosolic water volume of 2.72 μl/mg protein was used to calculate the concentrations. Free cytosolic ADP was calculated from the equilibrium of CK [apparent equilibrium constant ($K_{eq\text{-}CK}$) = $166 \times 10^{-0.87(pH-7)}$]. Free AMP concentration ([AMP]) was calculated as $[ADP]^2 \times K_{eq\text{-}AK}/[ATP]$ [using the adenylate kinase (AK) equilibrium constant ($K_{eq\text{-}AK}$) = 1.05 (31) and where brackets indicate concentration]. The free energy of ATP hydrolysis (A_{ATP}) was calculated as $A_{ATP} = A_0 + RT \times \ln[ATP]/[ADP] \times [P_i]$, where R is the gas constant and T is absolute temperature.

Kinetics of CK. CK forward flux (PCr→ATP) was assessed by time-dependent saturation transfer of γ-ATP under control as previously described (7, 46). Briefly, 24 scans of fully relaxed spectra (repetition time = 10 s) were acquired by blocks of 8 scans cycling three times through the whole protocol. Six spectra acquired with γ-ATP saturation (duration of 0–4 s) allowed measurement of the PCr relaxation time (T_{1PCr}) and the apparent rate constant of PCr→ATP (k_{for}). The average control T_{1PCr} values were similar in both groups [3.1 ± 0.5 and 3.2 ± 0.4 s in WT ($n = 12$) and α_2-KO ($n = 11$), respectively]. To reduce experimental time and because T_{1PCr} is unchanged by LFI, steady-state saturation of γ-ATP was applied in LFI. k_{for} was determined from the ratio $Mss/Mo = 1/(1 + k_{for} \cdot T_{1PCr})$ (Mss and Mo are magnetization of PCr in the presence and absence of a 4-s saturation of γ-ATP and $T_{1PCr} = 3.1$ s). PCr→ATP, the product of k_{for} and PCr concentration, was expressed in millimolar per second.

Glucose transport and phosphorylation was assessed by following the transport and phosphorylation of 2-deoxy-D-glucose (2DG; 5 mM) in the presence of pyruvate (5 mM). P_i (1 mM) was added to the perfusate to prevent phosphorus depletion occurring in this protocol. After 25 min of control perfusion, 2DG was infused and the rate of apparition of 2DG6P was assessed during 15 min (7 spectra).

LFI protocols. After 10 min of equilibration in isovolumic condition of work, the stability of metabolite content was checked for 15 min and CK flux was assessed by time-dependent saturation transfer followed by two control spectra. LFI was induced by reducing flow to 10% of its control (LFI_{10}) for 30 min to assess the time change of phosphorus metabolites and intracellular pH (pH_i). Metabolic steady state was reached after 12 min of LFI_{10}, and CK flux was measured by steady-state saturation transfer followed by two control spectra. Some of the hearts were freeze clamped to estimate AMPK phosphorylation. Low-ischemia flow was further reduced to 5% of control (LFI_5) for 15 min and restored to its control value for 35 min before freeze clamping (α_2-KO, $n = 6$; WT, $n = 6$). For the determination of ischemic glucose transport and phosphorylation, the same hearts used to determined control 2DG6P accumulation were submitted to LFI_{10} for 25 min (10 spectra) to assess ischemic stimulation in each individual heart. Hearts perfused in the presence of oleate were submitted to a reduction in flow down to 10% for 30 min (LFI_{10}), followed by 45 min of reperfusion.

Respiration and energetic yield. $\dot{V}O_2$ was measured in parallel experiments out of the magnet using the same LFI reperfusion protocol. $\dot{V}O_2$ (expressed as μmol $O_2 \cdot min^{-1} \cdot g$ wet wt^{-1}) was measured on line from the difference in oxygen content in incoming (aortic PO_2) and outgoing (pulmonary artery, venous PO_2) perfusate

Downloaded from journals.physiology.org/journal/ajpheart at Univ Catholique Louvain Bruxe (130.104.166.176) on August 18, 2020.

using oximeters (Stratkhelvin Institute, Glasgow, Scotland) and Clark electrodes equipped with fast O_2-permeable membranes in thermoregulated chambers. The energetic yield was estimated by analyzing the relationship of steady-state $\dot{V}O_2$ to RPP in the same protocol of ischemia-reperfusion (WT, $n = 6$; α_2-KO, $n = 6$). To assess a wider range of contractile performance, a group of 6 WT and 6 α_2-KO hearts was submitted to β-stimulation by stepwise increases in isoprenaline concentrations (10^{-10}, 10^{-9}, 3.16×10^{-9}, 10^{-8}, 3.16×10^{-8}, and 10^{-7} M). This group was perfused under constant pressure (75 mmHg) at a lower external calcium concentration (1 mM) to prevent calcium overload and fibrillation. Coronary flow was continuously measured by a T106 flowmeter equipped with a 1-N probe (Transonic System, Ithaca, NY). Steady-state values of RPP and $\dot{V}O_2$, obtained 10 min after the change in isoprenaline concentration, were used to estimate the energetic yield by the linear regression between $\dot{V}O_2$ and RPP.

Intrinsic contractile properties of myofilaments. Mouse hearts were perfused under control condition ($n = 4$) or submitted to 10-min global ischemia after stabilization ($n = 4$). Muscle fiber bundles were dissected from left ventricle papillary muscles in a relaxing solution [pCa (−log 1/calcium concentration) = 9; see solutions below], incubated for 45 min at 4°C with 1% Triton X-100 to solubilize the membranes, and transferred to relaxing solution at 4°C until use. For ischemic fiber preparation and experiments, the solutions contained okadaic acid (100 nM) to inhibit phosphatases. After connection to a force transducer (model AE 801; SensoNor Microelectroniks), sarcomere length was adjusted to slack length and stretched by 20%. All experiments were performed at 22°C. Solutions, prepared as previously described (47), contained (in mM) 10 EGTA, 30 imidazole, 30.6 sodium, 3.16 magnesium, and 0.3 DTT. Ionic strength was adjusted to 0.16 M with potassium acetate and pH to 7.1 with acetic acid. Relaxing solutions contained 3.16 mM MgATP and 12 mM PCr at pCa 9. Activating solutions contained the same metabolites, and pCa ranged from 9 to 4. Active force and sensitivity to calcium were determined under isometric conditions by stepwise decreases in pCa until maximum tension was reached. Rigor solutions contained ATP ranging from pMgATP 6 to 2.5 (−log 1/MgATP concentration) at pCa 9. Rigor force and sensitivity to ATP were assessed by stepwise decrease in pMgATP; MM-CK functional activity was assessed by the same protocol in the presence of 12 mM PCr to activate myofibrillar-bound CK.

Tension was expressed in millinewtons per millimeter squared, and data were fit with a nonlinear fit of the Hill equation (Microcal Origin software, version 6.0).

Expression and phosphorylation of AMPK. Freeze-clamped hearts were kept in liquid nitrogen until their homogenization in a lysate buffer, which contained 0.1% Triton X-100 and (in mM) 50 HEPES, 50 KCl, 1 EDTA, 1 EGTA, 5 β-glycerol phosphate, 1 orthovanadate, 1 DTT, 5 $NaPP_i$, 2 PMSF, and a cocktail of protease inhibitors (Calbiochem set V, EDTA free). Fifty micrograms of protein were used for Western blot detection of AMPK isoforms using the polyclonal phospho-AMPK-α (Thr^{172}) and AMPK-α-*pan* antibodies (Cell Signaling) diluted at 1:500 and 1:1,000, respectively. Samples were resolved by 8% SDS-PAGE, transferred to polyvinylidene difluoride membranes, which were blocked with 3% skimmed milk, and then probed overnight at 4°C with the antibody. Horseradish peroxidase-conjugated donkey anti-rabbit secondary antibody (Santa Cruz) was used for further detection by enhanced chemiluminescence (Amersham). Sample loading was confirmed by Coomassie dying of the gel after the transfer process. Quantification of signals was performed using the Quantity-One software from Bio-Rad, and arbitrary units were standardized by loading a standard sample in every separated gel. For GLUT1 and GLUT4 detection, 20 μg of protein of total conventional extracts were probed with polyclonal anti-GLUT1 and anti-GLUT4 antibodies (Chemicon) diluted at 1:1,000.

Statistical analysis. All results are means ± SE. The *t*-test was used to compare WT and α_2-KO. Variance analysis followed by a Student Newman Keuls test was used to compare control, LFI, and reperfusion in each group. A value of $P < 0.05$ was considered as significant.

RESULTS

Cardiac phenotype function and energetics of the α_2-KO hearts. As previously shown in younger mice (53), deletion of the α_2-subunit did not modify the expression of α_1-protein, the α_2-subunit was not detectable, and the total AMPK protein level was reduced by ~60% (not shown) in agreement with the known cardiac distribution of α-isoforms. The characteristics of the animals were similar, and no sign of cardiac hyper- or hypotrophy was found in the α_2-KO old mice (Table 1). Thus aging did not reveal morphological consequences of the α_2-AMPK deletion in contrast with other transgenic models (35).

The contractile parameters (LVDP, heart rate, RPP, and coronary pressure) were similar in AMPK α_2-KO and WT hearts in both the presence and absence of fatty acids (Table 1). The energetic status of the α_2-KO heart did not differ from that of the WT heart (Table 2), although a slight nonsignificant reduction in PCr could be observed in the former. ATP, P_i, pH_i, and the calculated indexes (free [ADP] and [AMP] and the free energy of ATP hydrolysis) were similar in both strains. $\dot{V}O_2$ was also similar under both constant flow and constant pressure perfusion conditions. However, glycogen content was about twofold lower in the α_2-KO than in WT hearts. Because a similar twofold difference was found in nonperfused frozen hearts (not shown), this confirms that the low-glycogen content was a direct consequence of the α_2 deletion. This shows that,

Table 1. *Comparison of the cardiac function of normoxic α_2-KO and WT hearts*

	WT, $n = 56$	α_2-KO, $n = 60$
Characteristics of the animals		
Age, mo	8.9±0.5	8.1±0.5
Body weight, g	36.5±0.9	35.2±0.7
Heart weight, g	0.29±0.01	0.28±0.01
Heart-to-body weight ratio, mg/g	7.9±0.2	7.9±0.2
	WT, $n = 24$	α_2-KO, $n = 19$
Cardiac function of the isolated heart perfused at constant flow in the presence of pyruvate and glucose		
LVDP, mmHg	71±4	71±4
Heart rate, beats/min	319±17	292±16
RPP, 10^4 mmHg·beats·min^{-1}	2.1±0.1	2.0±0.1
Coronary pressure, mmHg	103±8	112±9
EDP, mmHg	8±1	9±1
	WT, $n = 5$	α_2-KO, $n = 5$
Cardiac function of the isolated heart perfused at constant flow in the presence of oleate and glucose		
LVDP, mmHg	86±7	84±7
Heart rate, beats/min	358±18	367±11
RPP, 10^4 mmHg·beats·min^{-1}	3.2±0.1	3.5±0.2
Coronary pressure, mmHg	98±14	114±14
EDP, mmHg	9±1	10±1

Values are means ± SE; *n* is no. of hearts. Hearts were perfused at a constant flow of 2.5 ml/min either in presence of 2 mM pyruvate and 11 mM glucose or in presence of 0.4 mM oleate prebound to 1% BSA and 5 mM glucose as substrates. WT, wild type; α_2-KO, α_2-AMP activated protein kinase knockout; HR, heart rate; LVDP, left ventricular developed pressure; EDP, end-diastolic pressure; RPP, rate pressure product.

Downloaded from journals.physiology.org/journal/ajpheart at Univ Catholique Louvain Bruxe (130.104.166.176) on August 18, 2020.

Table 2. *Energetic parameters of the basal control WT and α_2-KO hearts*

	WT, $n = 12$	α_2-KO, $n = 11$
ATP, mmol/l	8.6±0.3	8.4±0.2
PCr, mmol/l	16.2±0.7	14.4±0.6
P_i, mmol/l	4.0±0.5	3.6±0.4
PCr/ATP	1.9±0.1	1.7±0.1
pH_i	7.09±0.02	7.08±0.01
ADP, μmol/l	59±7	68±6
A_{ATP}, kJ/M	−56.2±0.4	−56.0±0.5
AMP, μmol/l	0.48±0.10	0.76±0.22
AMP/ATP × 10^5	0.56±0.11	0.64±0.08
Glycogen, μmol glucosyl unit/g frozen wt	12.2±0.8	5.5±0.7*

Values are means ± SE. ATP, phosphocreatine (PCr), P_i, and intracellular pH (pH_i) were measured from ^{31}P-NMR spectroscopy after 30-min equilibration in normoxic perfusate containing pyruvate and glucose using the ATP measured biochemically as standard. Correction from partial saturation of NMR signal due to incomplete magnetization relaxation was applied. Free ADP, free AMP, and free energy of ATP hydrolysis (A_{ATP}) were calculated using the equilibrium constant of creatine kinase and adenylate kinase. No significant difference was found in any of the energetic parameters except for the glycogen content [measured in WT ($n = 4$) and α_2-KO ($n = 5$) and expressed per g frozen wt]. *Significantly different from WT, $P < 0.001$.

apart from decreasing the glycogen reserve, the deletion of the catalytic α_2-subunit had no major effect on the normoxic contractile respiratory and energetic status.

Contractile and metabolite changes in LFI and reperfusion. The acceleration of the global ischemic contracture that our group recently reported in the α_2-KO (53) could result from a defect in the anaerobic ATP synthesis pathways (glycolytic or glycogenolytic) and/or in the energy transfer or buffering by CK. Indeed, both events inhibited the myofibrillar ATPase activity by increasing local [ADP] (47). To understand the factors contributing to the acceleration of the ischemic contracture, we used a model of partial ischemia, reducing flow to 10% (LFI_{10}) and then to 5% (LFI_5) of its control value, and followed the time course changes in phosphorylated compounds and pH_i in WT and α_2-KO hearts. In the presence of glucose and pyruvate as substrate, LFI_{10} induced an immediate drop in RPP (resulting from both decreased left ventricle systolic-developed pressure and heart rate; not shown), similar in WT and α_2-KO (Fig. 1). EDP rose in four of nine α_2-KO hearts but in none of the WT hearts. Because of the variability of the EDP rise in the α_2-KO heart, the average EDP during moderate LFI_{10} was not significantly different in both groups.

In terms of phosphorus compounds, the onset of LFI_{10} resulted in an immediate drop in PCr concentration followed by the establishment of a new steady state after ~10 min (allowing measurement of CK flux). Steady-state PCr concentration was not significantly different in α_2-KO and WT hearts (Fig. 1), although its percent decrease was less pronounced in α_2-KO (down to 38 ± 5% and 55 ± 4%, $P < 0.05$, respectively; Fig. 2). [ATP] decreased monotonously to ~70% of its control value in both strains, and a similar moderate acidosis occurred (pH_i was 6.87 ± 0.05 in α_2-KO and 6.91 ± 0.09 in WT; not significant). Despite these discrete changes, the PCr-to-ATP ratio was less affected by ischemia in α_2-KO than in WT (1.38 ± 0.05 and 0.92 ± 0.09, respectively; $P < 0.001$), and thus the free [ADP] increased largely in WT (146 ± 21 μM) compared with α_2-KO (82 ± 6 μM, $P < 0.01$; Fig. 2). Free [AMP] rose ~2-fold in α_2-KO compared with 12-fold in WT (to 1.4 ± 2 and 4.4 ± 0.9 μM, respectively; $P < 0.01$). Free [AMP]-to-[ATP] ratios increased by 3- and 17-fold, respectively. The glycogen content measured at the end of LFI_{10} was significant lower in α_2-KO than in WT (3.4 ± 0.8 and 9.7 ± 1.5 μmol glucosyl units/g frozen wt; $P < 0.01$). From remnant pyruvate oxidation, glycogen depletion was modest, and the rate of its utilization appears similar in both groups (~0.12 μmol glucosyl unit·g frozen $wt^{-1}\cdot min^{-1}$).

To increase the metabolic challenge, flow was further reduced to 5% of control (LFI_5). A significant ischemic contracture developed in all α_2-KO hearts but only in one of the WT: the average EDP rose by 28 ± 8 and 5 ± 2 mmHg, respectively, at the end of the 15-min LFI_5 period ($P < 0.05$, Fig. 1). Metabolic changes were exacerbated in both α_2-KO and WT, but lower [ATP] and pH_i occurred in α_2-KO (Figs. 1 and 2). As for moderate LFI_{10} ischemia, both the accumulation of ADP and AMP and the increase in AMP-to-ATP ratio were much lower in the α_2-KO than in the WT hearts (Fig. 2). For example, free [AMP] rose to 1.8 ± 0.2 μM in α_2-KO vs. 6.7 ± 1.6 μM in WT ($P < 0.01$). The lower content in the adenylate phosphate pool observed in the α_2-KO suggests a larger cellular efflux of adenylate moieties in the α_2-KO heart.

Upon reperfusion, EDP further rose in both strains. Despite the exacerbation of ischemic contracture, postischemic systolic activity recovered to similar levels in both α_2-KO and WT (to ~60% of control; Fig. 1). ATP recovery was insignificant, as expected from the leakage of purine bases occurring during ischemia and from the slow rate of purine biosynthesis in the myocardium. The time course of PCr and pH_i recovery appeared slower in α_2-KO than in WT. At the end of reperfusion period, the [ATP], the sum of adenylate phosphates, and pH_i were significantly lower in α_2-KO than in WT and did not recover to their control value in α_2-KO hearts. AMP recovery was complete in both strains. The ischemia-recovery protocol induced similar leakage of cytosolic enzymes (LDH and AK) in both strains, whereas the mitochondrial citrate synthase activity was unchanged (Table 3).

CK activity and flux. To understand whether alterations of CK fluxes participate in the early development of contracture, CK function was evaluated. The specific activity of the enzymes involved in energy transfer (CK and AK) was unaltered by the α_2 deletion (Table 3). The unidirectional PCr→ATP flux was measured by ^{31}P NMR saturation transfer in control and LFI_{10} (Fig. 3*A*). In control, k_{for} and PCr→ATP were similar in α_2-KO and WT (average PCr→ATP of ~8.5 mmol/s). LFI_{10} induced a similar 50% impairment of CK flux in both strains. The decrease in CK-specific activity was expected from the well-known leakage of cytosolic CK at reperfusion (Table 3). Thus the deletion of the α_2-AMPK did not no alter global control and ischemic CK fluxes, suggesting that the regulation of CK is not critically dependent on the presence of α_2-AMPK isoform or on the ischemic stimulation of AMPK activity.

However, the preservation of global CK flux does not imply unaltered subcellular CK function (23). Indeed, the MM-CK isoform bound to the myofilaments functions to control the local [ADP] responsible for the formation of rigor bonds in ischemia (48). Because AMPK colocalizes with MM-CK in myofibrils and was earlier suggested to control its activity by phosphorylation (37), the absence of the α_2-isoform could directly affect the rigor properties of the myofibrils. The

Downloaded from journals.physiology.org/journal/ajpheart at Univ Catholique Louvain Bruxe (130.104.166.176) on August 18, 2020.

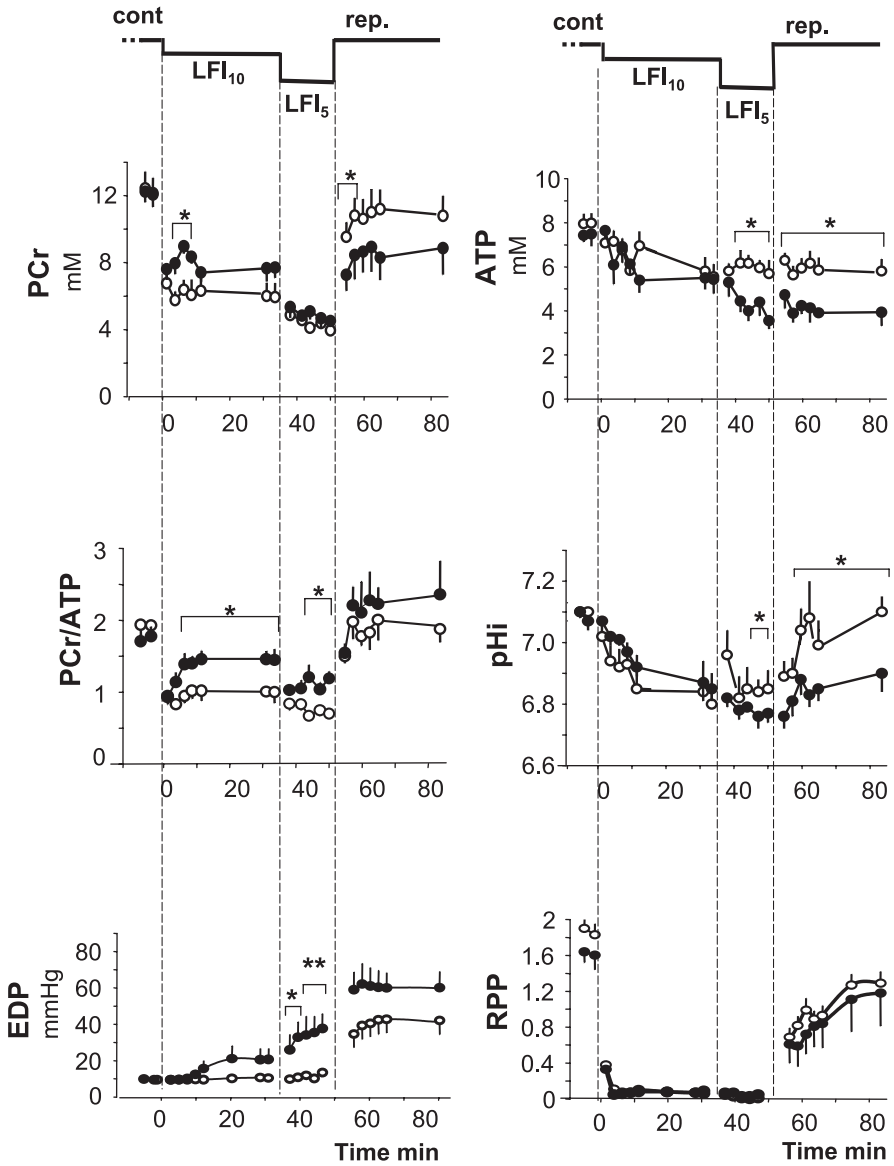

Fig. 1. Time-dependent response to a low-flow ischemia (LFI) and reperfusion protocol in the absence of fatty acids: contractility and NMR-measured phosphorus compounds. *Top* and *middle*: NMR-measured parameters showing concentrations of PCr and ATP (*top*) and ratio of PCr to ATP and intracellular pH (pH_i; *middle*). *Bottom*: mechanical activity showing end-diastolic pressure (EDP) and rate pressure product (RPP; in 10^4 mmHg·beats·min^{-1}). LFI was induced by reducing flow to 10% of its control (LFI_{10}) for 30 min ($n = 9$); LFI was further reduced to 5% of control (LFI_5) for 15 min ($n = 6$). Cont, control flow [wild-type (WT) hearts, $n = 12$; α_2-AMP-activated protein kinase (AMPK) knockout (α_2-KO) hearts, $n = 11$]; rep, reperfusion in control flow ($n = 6$). ○, WT; ●, α_2-KO. Substrates were 2 mM pyruvate and 5 mM glucose. *Significant difference between α_2-KO and WT ($P < 0.05$) (for clarity, the difference with the control value is not shown; see RESULTS).

consequence of the α_2 deletion on the activity of MM-CK and the rigor properties of the myofibrils were assessed in Triton X-100-skinned fibers isolated from normoxic or ischemic-perfused hearts. Figure 3*B* shows the rigor force induced by decreasing MgATP concentration and the sensitivity to ATP (characterized by $pMgATP_{50}$, the pMgATP inducing half rigor force development). The sensitivity to ATP of the rigor force was unaffected by α_2 deletion ($pMgATP_{50}$ was similar in WT and α_2-KO; Table 4). An index of the functional activity of MM-CK activity bound in the vicinity of the ATPase is the shift in the apparent $pMgATP_{50}$, induced by addition of PCr (49). The addition of PCr induced a similar shift of $pMgATP_{50}$ in WT and α_2-KO (Fig. 3*B* and Table 4), showing that the absence of α_2-AMPK did not modify the functional activity of myofibrillar-bound CK. Contractile properties of fibers isolated from ischemic WT and α_2-KO were similar to those of their normoxic control (not shown). In conclusion, our results show that the acceleration of the ischemic contracture in the α_2-KO is not due to an inhibition of the energy transfer and/or buffering by CK or to an alteration of the function of MM-CK bound in the vicinity of myofibrils.

Glucose uptake and phosphorylation. Because AMPK, as a metabolic switch, is involved in the control of glucose metabolism under stress, we assessed the consequence of α_2 deletion on glucose transport and phosphorylation by following the phosphorylation rate of 2DG by ^{31}P-NMR spectroscopy in control and under LFI_{10}. Figure 4*A* presents a series of spectra obtained from representative WT and α_2-KO hearts perfused at normal flow before (*spectrum a*) and at various times after the addition of 5 mM 2DG (*spectra b–d*). Figure 4*B* shows the time course of 2DG6P accumulation in α_2-KO and WT hearts and the contractile activity in control flow and in LFI_{10}. In both WT and α_2-KO, normoxic infusion of 2DG did not alter contractility due to the presence of pyruvate, which bypasses the early steps of glycolysis and fuels the mitochondria as originally described (22). In control flow, the accumulation of 2DG6P was slow in α_2-KO compared with WT. As shown in Fig. 4*C*, the average rate of 2DG6P accumulation was threefold

Downloaded from journals.physiology.org/journal/ajpheart at Univ Catholique Louvain Bruxe (130.104.166.176) on August 18, 2020.

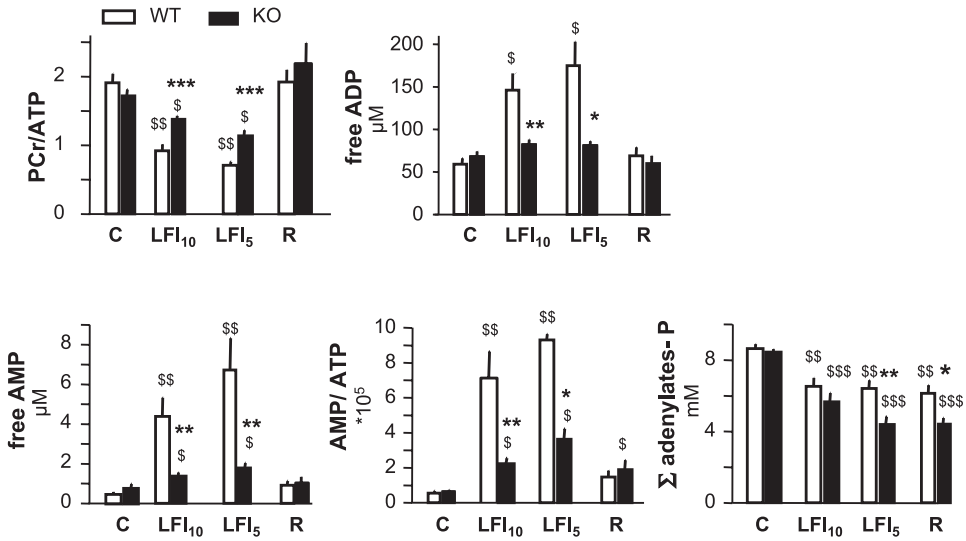

Fig. 2. Steady state of metabolites in LFI and reperfusion (R). Steady state was average of the last 2 spectra in each perfusion condition in hearts of Fig. 1. C, control; PCr, phosphocreatine; Σ adenylates-P, sum of adenylate phosphates (ATP + ADP + AMP). Significant difference between WT and α_2-KO: $^*P < 0.05$, $^{**}P < 0.01$, $^{***}P < 0.001$. Significantly different from the respective control group: $\$P < 0.05$, $\$\$P < 0.01$, $\$\$\$P < 0.001$.

slower in α_2-KO than in WT (0.2 ± 0.1 and 0.6 ± 0.1 nmol·min^{-1}·mg protein^{-1}, respectively; $P < 0.05$). Each individual heart was then subjected to 15 min of LFI_{10}. The rate of 2DG6P accumulation increased in both strains, albeit to a lower level in α_2-KO than in WT (0.6 ± 0.2 and 1.5 ± 0.2 nmol·min^{-1}·mg protein^{-1}, respectively; $P < 0.01$) (see Fig. 4 legend for details of measurement). Notice, however, that the threefold ischemic stimulation of 2DG transport and phosphorylation were similar in both mouse models (Fig. 4*C*). The defect in glucose transport and/or phosphorylation in the control α_2-KO is not due to a reduction in the expression of glucose transporters GLUT1 and GLUT4 (Fig. 4*D*). Thus the α_2-AMPK isoform is required for a normal glucose uptake and glycogen content under normoxic condition, although the stimulation of glucose uptake occurring during ischemia seems to be independent of the presence of the α_2-isoform. In conclusion, both the impaired glucose transport and phosphorylation and the low content in glycogen could account for the early rise in ischemic contracture of the heart deleted in α_2-AMPK.

Phosphorylation of AMPK. Figure 5*A* shows Western blots of total AMPK and AMPK phosphorylated in WT and α_2-KO hearts under control conditions and with stimulation of phosphorylation by LFI_{10} (in both the presence and absence of 2DG). In control conditions, a very low basal phosphorylation of total AMPK was found in α_2-KO compared with WT. LFI_{10} significantly increased AMPK phosphorylation in both α_2-KO and WT (Fig. 5*C*). However, phosphorylation of AMPK by LFI_{10} was threefold lower in α_2-KO than in WT and sixfold lower in LFI in the presence of 2DG. On reperfusion, AMPK phosphorylation decreased in both strains, remaining slightly higher than control in the α_2-KO.

Energetic cost of contraction. To understand how the contractility of the α_2-KO heart can be similar to that of a WT heart, we assessed their energetic cost of contraction. Indeed, one of the strategies of the myocardium submitted to a chronic stress is to improve the economy of its contraction (42). $\dot{V}O_2$ was continuously measured in a protocol of LFI-reperfusion performed out of the magnet (Fig. 6*A*). Contractile response, RPP, and rise in EDP were similar to those described in Fig. 1. $\dot{V}O_2$ in basal condition, although slightly lower in α_2-KO, was not significantly different from WT (5.1 ± 0.4 and 6.6 ± 0.6 µmol O_2·min^{-1}·g wet wt^{-1}, respectively). $\dot{V}O_2$ values during LFI_{10}, LFI_5, and reperfusion were also similar in both strains. The energetic cost of contraction (estimated by the slope of the relationship between $\dot{V}O_2$ and contractility) tended to be lower in α_2-KO than in WT, but the difference did not reach significance. To analyze more precisely this relationship, higher contractile performances were induced by β-stimulation. Because perturbation of the urinary excretion of catecholamines was previously described in this model (50), we first verified that the α_2 deletion did not alter the response of the myocardium to catecholamines. The sensitivity to isoprenaline was similar in both strains, as shown in Fig. 6*B* (pooled value of $EC_{50} = 4.9 \pm 0.5\ .10^{-9}$ M isoprenaline). Maximal stimulation, obtained in the presence of 3.10^{-8} M isoprenaline, resulted in nonstatistically different values of RPP (10.3 ± 0.7 and 8.3 ± 0.8 10^4 mmHg·beats·min^{-1} in α_2-KO and WT, respectively) and $\dot{V}O_2$ (18.5 ± 2.9 and 20.5 ± 2.5 µmol O_2·min^{-1}·g wet wt^{-1}). This shows that the α_2-KO heart perfused in the presence of glucose and pyruvate was not limited in its energy production. However, the energetic cost of its contraction, estimated from the slope of the linear relationship between $\dot{V}O_2$ and RPP, was significantly lower than in a WT heart (Fig. 6*C*; average slope of 1.50 ± 0.09 and 2.26 ± 0.17 in α_2-KO and

Table 3. *Enzymatic activities*

	Control		Reperfusion	
	WT, $n = 3$	α_2-KO, $n = 3$	WT, $n = 7$	α_2-KO, $n = 5$
Creatine kinase	507±39	669±47	273±47*	258±39*
Adenylate kinase	370±12	389±9	116±16*	104±9*
Citrate synthase	150±17	133±6	137±10	140±15
LDH	203±19	211±15	118±8*	104±9*

Values are means ± SE, expressed in IU/g frozen wt. Data are from freeze-clamped hearts. Control results were obtained after 20 min of basal perfusion. Reperfusion results were obtained 35 min after low-flow ischemia was reduced to 10% (LFI_{10}) and then to 5% (LFI_5) of control values (hearts of Fig. 1). LDH, lactate dehydrogenase. *Significantly different from control, $P < 0.05$. There was no significant difference between WT and α_2-KO for any variable.

Downloaded from journals.physiology.org/journal/ajpheart at Univ Catholique Louvain Bruxe (130.104.166.176) on August 18, 2020.

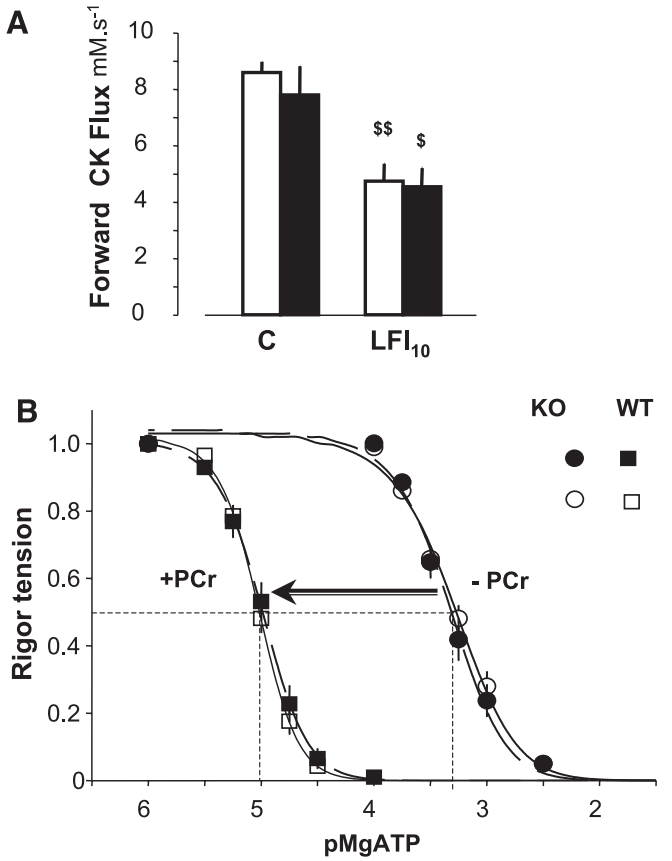

Fig. 3. Creatine kinase (CK) function. *A*: ^{31}P-NMR-measured forward CK flux during metabolic steady state under control flow (C, $n = 11$) and LFI_{10} ($n = 9$) in WT (open bars) and α_2-KO (closed bars) hearts. Significant difference from control group: $\$P < 0.05$, $\$\$P < 0.01$. *B*: functional activity of myofibrillar MM-bound CK. Sensitivity of the rigor tension to ATP was similar in Triton X-100-treated fibers of α_2-KO and WT hearts; half-maximum rigor tension occurred at similar pMgATP. The efficiency of MM-bound CK (arrow), estimated from the shift in the apparent sensitivity to MgATP induced by the addition of 12 mM PCr (+PCr, squares), was similar in both strains (see Table 4 for mean data). −PCr, without PCr (circles).

WT, respectively; $P < 0.05$). This suggests that the α_2-AMPK deletion resulted in an improvement in the economy of contraction.

To improve the economy of contraction, a rodent heart under chronic stress expresses the slow isoform of myosin-ATPase, which consumes less ATP per force unit, or might change the activation properties of its ATPase. However, the isomyosin profile of the WT shows a pure V1 phenotype (100% fast type, $n = 9$ WT) as expected in a mouse heart, and this profile was unaltered by the α_2-AMPK deletion ($n = 8$ α_2-KO). The active tensions and the calcium sensitivities of the ATPase studied in Triton X-100-skinned fibers are shown in Table 4. Both the

Table 4. *Intrinsic contractile properties of the myofilaments*

	WT ($n = 9$)	α_2-KO ($n = 9$)
Fiber diameter, μm	239±17	215±10
Calcium-activated force		
Resting force, mN/mm^2	3.8±0.6	4.0±0.7
Active force, mN/mm^2	34.2±2.4	32.3±1.7
pCa_{50}	5.55±0.03	5.64±0.03
n_H	2.90±0.10	2.67±0.08
Rigor force		
$pMgATP_{50}$	3.28±0.05	3.30±0.05
$pMgATP_{50}$ + PCr	5.03±0.03	4.98±0.05
MM-CK efficacy	1.73±0.05	1.68±0.06

Values are means ± SE. pCa_{50}, pCa leading to half of the maximum active force; n_H, Hill coefficient; $pMgATP_{50}$ and $pMgATP_{50}$ + PCr, pMgATP needed to develop half of the rigor force (in the absence and in the presence of 12 mM PCr, respectively). MM-CK efficacy = [($pMgATP_{50}$ + PCr) − $pMgATP_{50}$], that is, the shift in the apparent sensitivity to MgATP induced by creatine kinase (CK) activation.

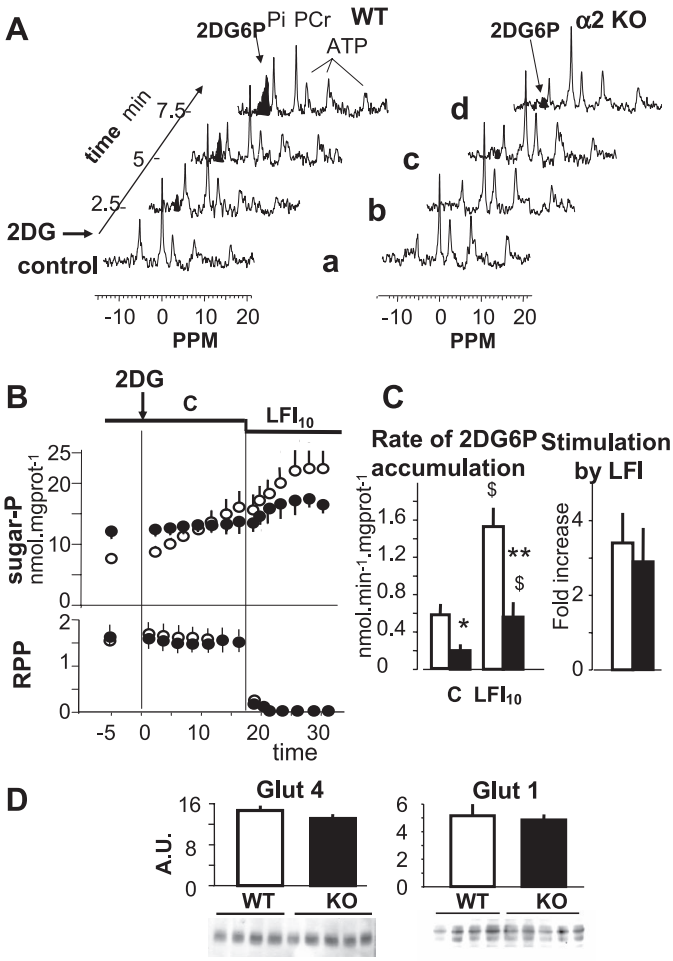

Fig. 4. ^{31}P-NMR estimation of the glucose transport and phosphorylation and its stimulation by LFI. *A*: stacked plot of NMR spectra showing the accumulation of 2-deoxy-D-glucose-6-phosphate (2DG6P) as a function of time in representative WT (*left*) and α_2-KO (*right*) hearts. *Spectrum a*, control; *spectra b–d* were acquired during infusion of 2-deoxy-D-glucose (2 DG; 5 mM) 2.5, 5, and 7.5, min, respectively, after the start of infusion. Acquisition time was 5 min for each spectrum. Substrate was 2 mM pyruvate in presence of external 1 mM P_i. *B*: time evolution of sugar phosphate (sugar-P) content and contractility on addition of 5 mM 2DG. *Top*: accumulation of 2DG6P as a function of time in α_2-KO (●; $n = 6$) and WT (○; $n = 7$) hearts. 2DG infusion was started at *time 0* in control flow; LFI_{10} was induced in the presence of 2DG after 17.5 min of control flow. *Bottom*: contractility (RPP in 10^4 mmHg·beats·min^{-1}) was unaffected by 2DG infusion in control flow in both α_2-KO and WT hearts and dropped similarly in LFI. *C*: rate of 2DG6P accumulation in control and LFI. *Left*: average rate of 2DG6P accumulation was slower in α_2-KO than in WT both in control flow and under LFI_{10}. Rate of 2DG6P accumulation in LFI was estimated from the first 10 min of ischemia (4 spectra). Significant difference between α_2-KO and WT: $*P < 0.05$, $**P < 0.01$. Significantly different from control: $\$P < 0.05$. *Right*: stimulation of 2DG transport and phosphorylation by LFI_{10} was similar in α_2-KO and WT (expressed as fold increase in 2DG6P rate of accumulation induced by LFI_{10} for each individual heart). *D*: expression of GLUT1 and GLUT4 protein. AU, arbitrary unit. *Bottom* shows Western blot analysis. For WT and α_2-KO, $n = 7$.

Downloaded from journals.physiology.org/journal/ajpheart at Univ Catholique Louvain Bruxe (130.104.166.176) on August 18, 2020.

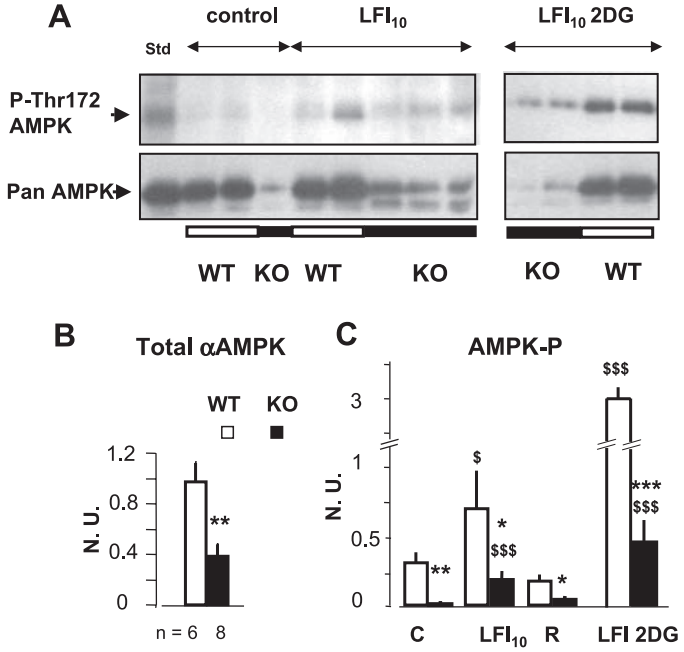

Fig. 5. AMPK and its phosphorylation in LFI in WT and α_2-KO hearts. *A*: Western blot showing total AMPK protein and its phosphorylation (P) at Thr^{172} in control condition and in LFI_{10} in absence (*left*) and presence of 2DG (*right*). Std, standard: rat heart after 10 min of global ischemia. *B*: total AMPK protein in WT and α_2-KO hearts. *C*: average level of phosphorylation of total AMPK (AMPK-P) in control condition (C; for WT and α_2-KO, $n = 4$) and in LFI_{10} for 30 min (for WT and α_2-KO, $n = 7$). R, 35 min after reperfusion (for WT, $n = 4$; for α_2-KO, $n = 3$); LFI 2DG, 15 min of 2DG + LFI_{10} for 15 min (for WT, $n = 5$; for α_2-KO, $n = 6$). NU, normalized unit (AMPK-P normalized to AMPK-P of the standard). Significantly different from control: $\$P < 0.05$, $\$\$\$P < 0.001$. Significant difference between α_2-KO and WT: $*P < 0.05$; $***P < 0.001$.

maximal active tension of myofibrils (at pCa 4.5) and the sensitivity of myofibrillar ATPase to calcium activation were similar in α_2-KO and WT (pCa_{50} was 5.64 ± 0.03 in α_2-KO and 5.55 ± 0.03 in WT; not significant). In conclusion, the improvement in the economy of contraction observed in α_2-KO did not result from adaptations of the myofibrils.

Contractile consequence of α_2 deletion in the presence of fatty acids. The early development of the ischemic contracture in the α_2-KO observed in the absence of fatty acids (Fig. 1) was also evidenced in their presence (Fig. 7): ischemic contracture developed after 4.9 ± 1.1 and 23 ± 3 min in α_2-KO and WT, respectively ($P < 0.01$). Maximal EDP rise was higher in α_2-KO than in WT (EDP rose by 65 ± 21 and 11 ± 8 mmHg, respectively; $P < 0.05$). As expected, the presence of fatty acids exacerbated the contracture in the α_2-KO (comparison with Fig. 1 shows significantly higher maximal EDP value in the presence of fatty acids; $P < 0.05$). In contrast with the similarity of postischemic recovery observed with pyruvate (Figs. 1 and 5), the recovery was delayed in the α_2-KO in the presence of oleate. During the first 20 min of reperfusion, left ventricular-developed pressure and RPP were significantly lower in the α_2-KO than in WT (Fig. 7; $P < 0.05$), although they later reached similar values (after 40 min of reperfusion, RPP recovered to 62 ± 6% and 74 ± 7% of their respective control values in α_2-KO and WT; not significant). In addition, EDP recovery was poor in the α_2-KO heart. This shows a specific implication of the α_2-AMPK isoform in the preservation of the early reperfusion contractile performance in the presence of fatty acids.

DISCUSSION

The basal cardiac energetic status, contractility, and respiration are unaffected by α_2-AMPK deletion. We found a dual effect of the α_2-AMPK deletion on the contractile and metabolic responses of the myocardium submitted to an LFI-reperfusion episode. We confirm that the heart of the α_2-KO mouse is more susceptible to development of an ischemic contracture. We show that this acceleration of contracture can be explained by a deficit in energy synthesis resulting from both a constitutive impairment of glycogen stores and a de-

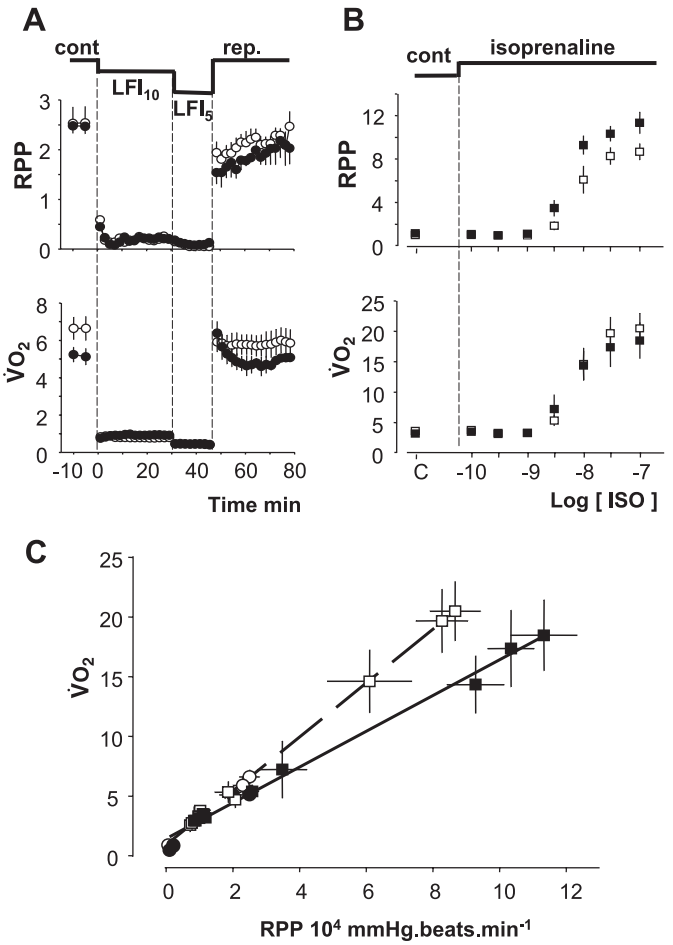

Fig. 6. Oxygen consumption ($\dot{V}O_2$) and the economy of contraction. *A*: LFI and reperfusion protocol. RPP are in 10^4 mmHg·beats·min^{-1}. $\dot{V}O_2$ are in μmol O_2·min^{-1}·g wet wt^{-1}. EDP changes were similar to Fig. 1*A*. ○, WT ($n = 6$); ●, α_2-KO ($n = 6$). *B*: response of α_2-KO and WT hearts to a β-stimulation induced by increasing concentrations of isoprenaline ranging from 10^{-10} to 10^{-7} M. Steady-state values were obtained 10 min after the change in isoprenaline concentration. □, WT ($n = 6$); ■, α_2-KO ($n = 6$). *C*: energy cost of contraction estimated from the linear relationship between $\dot{V}O_2$ and RPP for both protocols. Data included both LFI and isoprenaline protocols. Average linear regressions were described by $y = 2.26$ (SE = 0.17)$x + 0.91$ (SE = 0.32), $r^2 = 0.9967$, in WT and by $y = 1.50$ (SE = 0.09)$x + 1.43$ (SE = 0.18), $r^2 = 0.9907$, in α_2-KO (where y is $\dot{V}O_2$ and x is RPP). *t*-Test analysis (performed on the individual relationship of each heart) showed that the slope of α_2-KO was significantly lower than that of the WT ($n = 12$ for WT and for α_2-KO; $P = 0.03$), whereas the ordinate at origin was not significantly different.

Downloaded from journals.physiology.org/journal/ajpheart at Univ Catholique Louvain Bruxe (130.104.166.176) on August 18, 2020.

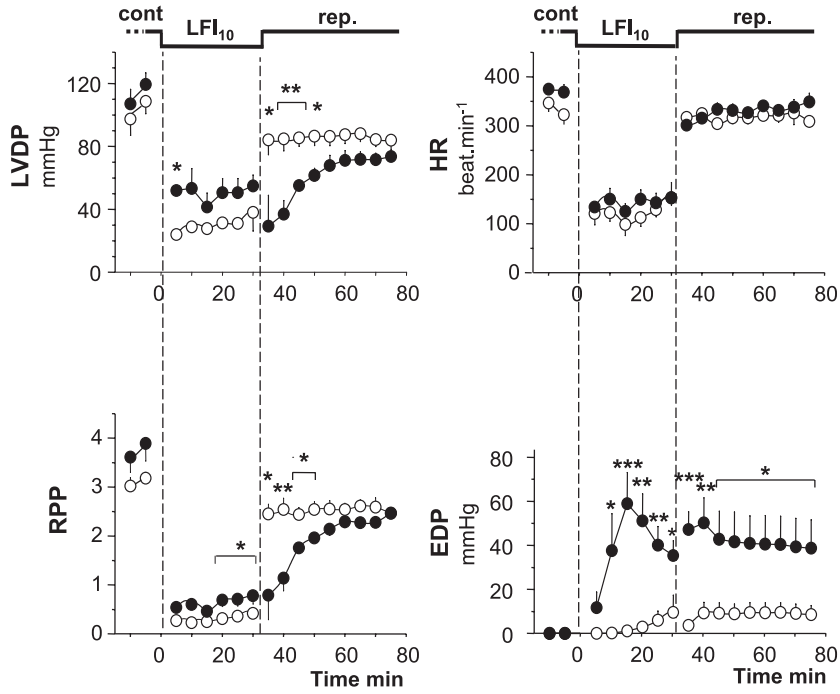

Fig. 7. Contractile response to a LFI and reperfusion protocol in the presence of fatty acids. *Top*: left-ventricular developed pressure (LVDP) and heart rate (HR). *Bottom*: RPP (in 10^4 mmHg·beats·min^{-1}) and rise in EDP. ○, WT ($n = 5$); ●, α_2-KO ($n = 5$). Substrates were 0.4 mM oleate and 5 mM glucose. Significant difference between α_2-KO and WT: $*P < 0.05$, $**P < 0.01$, $***P < 0.001$.

creased glucose uptake and phosphorylation and not by an impairment of energy transfer. The unaltered energy transport by CK and function of the MM-CK suggest that the α_2-AMPK does not control CK in the myocardium. A novel finding is that the α_2-AMPK deletion does not affect the postischemic contractile function in the absence of fatty acids but reduced early contractile recovery in their presence.

Contractility and energetics of the normoxic heart. Despite the threefold decrease in glucose uptake and phosphorylation observed in the presence of pyruvate (Fig. 4, *B* and *C*), the α_2-AMPK deletion did not induce contractile defect as also observed ex vivo and in vivo in the same transgenic model (53). This shows that the presence of α_2-AMPK isoform is needed for optimal normoxic glucose transport and phosphorylation, although it is not required for the expression of GLUT transporters (Fig. 4*D*). The similarity of the energy status of the α_2-KO and WT heart indeed shows that the balance of energy utilization and synthesis is hardly affected by α_2 deletion: thus the α_2-KO heart is not an energetically starved myocardium. One could argue that the contractility of the isolated isovolumic perfused heart is low compared with the condition prevailing in vivo. However, steady-state high levels of contractility (similar to that of a WT heart) can be supported even at maximal levels of β-stimulation when pyruvate and glucose are available (Fig. 5), although the maximal activity of the complex I is impaired in the α_2-KO mitochondria (4). A novel interesting observation is that the α_2-deletion induced an increase in the economy of contraction. This does not result from the usual strategies developed by the pathological rodent heart, which tends to reduce the cost of its myofibrillar ATPase by expression of a slow-type myosin. We showed that the α_2-AMPK is not involved in the expression of myosin or regulatory contractile proteins (as suggested by the similarity of calcium sensitivity of the myofibrillar ATPase). Further investigation is needed to understand whether the economical contraction of the α_2-KO results from a modification in calcium homeostasis, excitation contraction coupling, and/or mitochondrial efficiency.

α_2-AMPK protects the heart from the ischemic contracture. LFI differs from global ischemia in two major ways. Degradation products (mainly lactate, protons, adenosine) are washed out of the cell, enabling continuation of glycolytic ATP production; however, because of the remnant oxygen supply, mitochondrial substrate oxidation still occurs. Indeed, a 30-min period of flow restriction down to 10% induced a moderate decrease in PCr, ATP, and pH_i [as previously reported in the rat heart (9)] and rapidly resulted in a new metabolic and contractile steady state in both WT and α_2-KO. The increased susceptibility for the development of an ischemic contracture observed in no flow ischemia (53) was also evident in our low-flow model (Fig. 1*A*). The ischemic contracture results mostly from an imbalance of the energy homeostasis leading to accumulation of ADP at the level of myofibrils, inhibition of ATPase, and development of a rigor state (47). This imbalance in energy homeostasis can result from an increased energy demand, an impairment of energy transfer by CK, and/or a deficit in the anaerobic ATP synthesis pathways. The hypothesis of an increased energy demand is eliminated by the similarity of LFI contractility in α_2-KO and WT (Figs. 1 and 6*A*) and the absence of change in the intrinsic contractile properties of the myofibrils (Table 4). The similarity of the ischemic CK fluxes (Fig. 3*A*) eliminates the hypothesis of a deficit in energy transfer by CK. On the contrary, because AMPK has earlier been suggested to inhibit CK activity (37), lower phosphorylation of AMPK in the ischemic α_2-KO could have been expected to prevent the ischemic decrease in CK flux. However, this was not observed (Fig. 3*A*). Thus our results show that α_2-AMPK phosphorylation is not involved in the regulation of CK flux and, provided that the α_1-isoform is not specifically involved in this regulation, suggest a minor physiological importance of AMPK in the ischemic inhibition of CK fluxes.

Downloaded from journals.physiology.org/journal/ajpheart at Univ Catholique Louvain Bruxe (130.104.166.176) on August 18, 2020.

Surprisingly, LFI induced in the α_2-KO a high steady state PCr-to-ATP ratio, which prevented a major rise in cellular free [ADP] (and [AMP]) in LFI_{10}. This could have resulted from unbalanced subcellular CK fluxes. However, this hypothesis is not supported. Neither the expression of the MM, MB, BB, or mitochondrial isoforms of CK nor the coupling of MM-CK to myofibrillar ATPase (Fig. 3), nor that of mitochondrial CK to adenine nucleotide translocase (3), was altered by the α_2-AMPK deletion. The ischemic free [ADP] and [AMP], besides being controlled by CK and AK activities, also depend on the activity of the enzymes of the AMP degradation pathways (AMP deaminase and 5′-nucleotidase). Except in global ischemia, in which the degradation products cannot be extruded from the cell, an inhibition of respiration (by hypoxia, chemical inhibition, or LFI) releases purine bases in the cardiac effluent due to AMP hydrolysis, which rapidly follows the initiation of ATP depletion (10, 19). This mechanism is thought to be beneficial in short-term hypoxia (28). The sum of adenylate phosphates (ATP + ADP + AMP) was indeed significantly lower in α_2-KO than in WT hearts at the end of LFI (4.4 ± 0.4 vs. 6.4 ± 0.4 mM; $P < 0.01$). This suggests that the low cellular [ADP] and [AMP] found in the α_2-KO (Fig. 2) might result from an increase in the degradation pathways. It is thus an interesting possibility, which to our knowledge has not yet been explored, that the α_2-AMPK subunit might interfere with the regulation or the expression of enzymes involved in the AMP degradation pathways.

Thus, in the absence of alterations in energy utilization and transfer, the energetic imbalance mostly results from a deficit in energy synthesis. Indeed, decreases in both glycolytic and glycogenolytic ATP production accelerate the LFI contracture in the rat heart (13). Indeed, the deficit in glycogen storage (Table 2 and Ref. 53), rather than in its rate of LFI utilization, is involved in the early development of contracture (Fig. 4). Similar results were observed in the KD mutant, although unaltered glycogen stores but reduced ischemic mobilization was found in the dominant-negative mutation (39, 51). The increase in glucose transport being a primary component of the glycolysis stimulation by ischemia, the slower glucose transport and phosphorylation in LFI (Fig. 4), and the marked decrease in lactate production found in global ischemia (53) show that the α_2 deletion impairs anaerobic glycolysis. Because ischemia was still able to stimulate glucose uptake in α_2-KO (Fig. 3*B*), the α_2-isoform is not required for the ischemic stimulation of glucose transport and phosphorylation and the α_1-isoform is possibly responsible for this remaining stimulation. In conclusion, the decreased glycogen stores, the impaired glucose transport, and/or phosphorylation, both concurring to impair anaerobic ATP synthesis in the α_2-KO myocardium, show that the presence of α_2-AMPK is essential for the prevention of ischemic contracture.

α_2 Deletion does not impair ischemic and postischemic contractility when pyruvate is present. We chose to use pyruvate as substrate because its oxidation is efficient in LFI; it enhances cardiac efficiency and also acts as an antioxidant (33, 34). In terms of fuel utilization, pyruvate increases the activity of complex II and that of complex I by anaplerotic flux via oxaloacetate. Moreover, through its conversion to lactate, pyruvate could relieve glycolytic constraint due to NADH accumulation under ischemia (6). The antioxidant effect of pyruvate is well documented (33, 34), and pyruvate was shown to prevent cardiac dysfunction and AMPK activation induced by hydrogen peroxide in the isolated rat heart (32). Thus, although it might not reflect an in vivo situation, pyruvate allowed focusing our study on the role of α_2-AMPK in the glycolytic pathway, the energetic status, and the metabolic response of the heart to an LFI-reperfusion challenge in conditions that minimize the complex interference of free oxygen and nitrosyl radical production with AMPK activity.

A major novel observation is that, despite the acceleration of the ischemic contracture, the α_2-AMPK deletion did not exacerbate the contractile consequences of an ischemia reperfusion episode in the heart perfused with glucose and pyruvate. At first sight, surprisingly, the lack of correlation between ischemic contracture and contractile recovery at reperfusion is not new (13, 24, 25). Our results are in the same line: the α_2-AMPK deletion decreased glycogen and accelerated the contracture, but it did not affect postischemic contractile recovery. Besides, contractility is not related to the ATP level but to its turnover rate (5, 22, 36, 46). Thus, despite a lower ATP content at reperfusion, the similarity of postischemic contractility in α_2-KO and WT suggests similar recovery of ATP turnover. This is most probably related to the low cost of contraction in the α_2-KO in the presence of pyruvate and glucose. Because the isomyosin profile and the regulation by calcium of the active tension were similar in α_2-KO and WT hearts, this economical contraction does not originate from a lower ATP requirement of the myofibrillar ATPase but probably rather from an improvement in the ATP-generating steps. Several mechanisms could contribute to the higher efficiency of the mitochondria in α_2-KO. A shift in endogenous substrate utilization could increase the phosphate-to-oxygen ratio or the intrinsic properties of mitochondrial respiration could be altered (3). Finally, because high adenosine levels improve the economy of contraction (20), the depletion in adenylate phosphates in the ischemic α_2-KO could increase coronary adenosine, contributing to the low-cost contractility of the α_2-KO heart. Further work is required to test the origin of the energetic efficiency of the α_2-KO myocardium in the presence of pyruvate and glucose.

Activators of AMPK. As discussed in detail previously (53), the activation of AMPK is complex (2, 18, 41) and depends on a combination of phosphorylation by upstream kinases and AMP stimulation. In addition, kinetic activation by AMP depends on the type of α- and γ-isoforms composing the heterotrimer (1, 14, 45) and is antagonized by high [ATP]. The estimation of the [AMP] (and [ADP]) relevant for enzyme activation in a whole cell is not easy: the majority of the nucleotides are bound to intracellular compartments and metabolically inactive and their low concentrations prevent NMR detection (44). Alternatively, free [ADP] and [AMP] are calculated from the NMR-measured PCr, [ATP], and H^+ concentrations in the hypothesis of CK and AK equilibrium. Quasi-metabolic steady state is acceptable in our protocol because *1*) both CK flux (~8 mM/s) and AK flux (38) are at least 10^3 higher that the higher rate of ATP degradation (estimated from Fig. 1 in the ischemic α_2-KO to ~1.5 μM/s) and the V_{max} of enzymes involved in AMP degradation (21, 43) and *2*) CK and AK had similar specific activities in both WT and α_2-KO (Table 3). Indeed the free [AMP] increase observed in our LFI protocol (from 1.5 to 7 μM) is in the relevant range of AMPK activation found in vitro and in the perfused mouse heart (17,

Downloaded from journals.physiology.org/journal/ajpheart at Univ Catholique Louvain Bruxe (130.104.166.176) on August 18, 2020.

45). Obviously, lower level of AMPK phosphorylation in ischemia is expected from the 60% decrease in total AMPK induced by α_2 deletion. However, in all our experimental conditions, the phosphorylation of AMPK was related to the change in AMP-to-ATP ratio in both α_2-KO and WT (compare Figs. 2 and 5*C*). Under global ischemia, a lower level of AMPK activation was also found in the same α_2-KO heart, but the accumulation of AMP in α_2-KO was higher than in WT (53). Both results might appear at first sight contradictory, but this discrepancy is due to the difference between global ischemia, a close system where degradation products accumulate in the cell, and LFI, an open system resulting in metabolic steady state where AMP hydrolysis and washout of degradation products can occur.

Is AMPK involved in cardiac protection or in cardiac injury? The preservation of the postischemic contractile function in the α_2-KO with glucose and pyruvate (Fig. 1) suggests that α_2-AMPK isoform is not needed for the postischemic contractile recovery in the absence of fatty acids. In contrast, in the presence of fatty acids, in an experimental set up closer to an in vivo situation, contractile recovery was poor at the onset of reperfusion both in our α_2-KO (Fig. 7) and in the α-KD model (39). This is in agreement with the well-known deleterious effect of free fatty acids in the ischemia-reperfusion episode. Although a physiological substrate, long-chain fatty acids decrease cardiac efficiency, activate AMPK, and increase phosphorylation of acetyl-CoA carboxylase (8, 12, 26). Moreover, during reperfusion, it has been proposed that sustained activation of AMPK and inactivation of acetyl-CoA carboxylase mediate the acceleration of fatty acid oxidation and the uncoupling of glucose oxidation and glycolysis (29, 30). For these reasons, it is commonly assumed that AMPK should play a negative role during reperfusion by inducing this uncoupling (15). Our results show that the α_2-AMPK is involved in the postischemic contractile recovery in the presence of fatty acids, as already described in the KD model by Russell et al. (39), whereas this role is not evident in their absence. These results clearly show that studies on the role of AMPK on fatty acid metabolism during reperfusion should not simply concentrate on the regulation of the acetyl-CoA carboxylase or malonyl-CoA pathways. Further work is needed to understand whether these opposite results are due directly to altered postischemic activation of the fatty acids metabolic pathway, different accumulation of fatty acids, and/or to the antioxidant effect of pyruvate attenuating the massive reactive oxygen species production at reperfusion. Ischemia, as expected, phosphorylated α_1-AMPK and stimulated glucose uptake in our model of α_2-deletion (Figs. 4 and 5 and Ref. 53), as well as in the dominant-negative mutation (51), but failed to do so in the KD mutation. The reasons for this lack of activation are not obvious, but it is possible that the overexpression of inactive α-subunit perturbs the heterotrimer α-β-γ association and the ischemic activation of AMPK and participates in the more severe ischemic damage of the KD mutant. Here, we showed that the α_2-isoform is specifically implicated in the protection of the early reperfusion damage. The similarity of the contractility in late recovery in the α_2-KO and in WT heart does not favor the hypothesis of more severe long-term damage in the former, although we did not directly evaluate the apoptotic response in our model.

ACKNOWLEDGMENTS

The authors thanks R. Fischmeister (Director U-749 INSERM) for continuous and stimulating scientific support, C. Beauloye and L. Hue for stimulating criticisms, P. Grondin for help, A. Garnier and D. Fortin for help in developing Western blot analysis, and P. Lechene for adaptation of the perfusion setup of mouse heart to NMR.

GRANTS

This work is supported by Institut National de la Santé et de la Recherche Médicale, France, by a grant of the Fondation de France, by a grant from the Fonds National de la Recherche Scientifique et Médicale, Belgium, and by the European Commission (grant QLG1-CT-2001-01488). K. Carvajal was funded by Association Française contre les Myopathies, O. Szarszoi by a grant from ISHR, and E. Zarrinpashneh by the Fonds Spéciaux de Recherche, UCL, Belgium. L. Bertrand is a Research Associate of the Fonds National de la Recherche Scientifique, Belgium. R. Ventura-Clapier is a Centre National de la Recherche Scientifique employee.

REFERENCES

1. **Adams J, Chen ZP, Van Denderen BJ, Morton CJ, Parker MW, Witters LA, Stapleton D, Kemp B.** Intrasteric control of AMPK via the γ_1-subunit AMP allosteric regulatory site. *Protein Sci* 13: 155–165, 2004.
2. **Altarejos JY, Taniguchi M, Clanachan AS, Lopaschuk GD.** Myocardial ischemia differentially regulates LKB1 and an alternate 5′AMP-activated protein kinase kinase. *J Biol Chem* 280: 183–190, 2004.
3. **Athea Y, Veksler V, Viollet B, Garnier A, Vaulont S, Ventura-Clapier R.** Knock out of the α2 subunit of AMP activated protein kinase (AMPK) alters cardiac oxidative capacity and substrate utilization (Abstract). *Circulation* 108: 296, 2003.
4. **Athea Y, Viollet B, Mateo P, Rousseau D, Novotova M, Garnier A, Vaulont S, Wilding J, Grynberg A, Veksler V, Hoerter JA, Ventura-Clapier R.** AMP-activated protein kinase α_2 deficiency affects cardiac cardiolipin homeostasis and mitochondrial function. *Diabetes* 56; 786–794, 2007.
5. **Balschi JA, Shen H, Madden MC, Hai JO, Bradley EL, Wolkowicz PE.** Model systems for modulating the free energy of ATP hydrolysis in normoxically perfused rat hearts. *Mol Cell Cardiol* 29: 3123–3133, 1997.
6. **Bassenge E, Sommer O, Schwemmer M, Bunger R.** Antioxidant pyruvate inhibits cardiac formation of reactive oxygen species through changes in redox state. *Am J Physiol Heart Circ Physiol* 279: H2431–H2438, 2000.
7. **Bittl JA, Ingwall JS.** Reaction rates of creatine kinase and ATP synthesis in the isolated rat heart. A ^{31}P NMR magnetization transfer study. *J Biol Chem* 260: 3512–3517, 1985.
8. **Burkhoff D, Weiss RG, Schulman SP, Kalil R, Wannenburg T, Gerstenblith G.** Influence of metabolic substrate on rat heart function and metabolism at different coronary flows. *Am J Physiol Heart Circ Physiol* 261: H741–H750, 1991.
9. **Cave C, Ingwall JS, Friedrich J, Liao RL, Saupe KW, Apstein CS, Eberli FR.** ATP synthesis during low-flow ischemia: influence of increased glycolytic substrate. *Circulation* 101: 2090–2096, 2000.
10. **Chen WN, Hoerter JA, Guéron. M.** A comparison of AMP degradation in the perfused rat heart during 2-deoxy-D-glucose perfusion and anoxia. 1. The release of adenosine and inosine. *J Mol Cell Cardiol* 28: 2163–2174, 1996.
11. **Christian TF, O'Connor MK, Schwartz RS, Gibbons RJ, Ritman EL.** Technetium-99m MIBI to assess coronary collateral flow during acute myocardial infarction in two closed-chest animal models. *J Nucl Med* 38: 1840–1846, 1997.
12. **Clark H, Carling D, Saggerson D.** Covalent activation of heart AMP-activated protein kinase in response to physiological concentrations of long-chain fatty acids. *Eur J Biochem* 271: 2215–2224, 2004.
13. **Cross HR, Opie LH, Radda GK, Clarke K.** Is a high glycogen content beneficial or detrimental to the ischemic rat heart? A controversy resolved. *Circ Res* 78: 482–491, 1996.
14. **Daniel T, Carling D.** Functional analysis of mutations in the γ_2 subunit of AMP-activated protein kinase associated with cardiac hypertrophy and Wolff-Parkinson-White syndrome. *J Biol Chem* 277: 51017–51024, 2002.
15. **Dyck JR, Lopaschuk GD.** AMPK alterations in cardiac physiology and pathology: enemy or ally? *J Physiol* 574: 95–112, 2006.
16. **Folmes CD, Clanachan AS, Lopaschuk GD.** Fatty acids attenuate insulin regulation of 5′-AMP-activated protein kinase and insulin cardioprotection after ischemia. *Circ Res* 99: 61–68, 2006.

Downloaded from journals.physiology.org/journal/ajpheart at Univ Catholique Louvain Bruxe (130.104.166.176) on August 18, 2020.

17. **Frederich M, Balschi JA.** The relationship between AMP-activated protein kinase activity and AMP concentration in the isolated perfused rat heart. *J Biol Chem* 277: 1928–1932, 2002.
18. **Frederich M, Zhang L, Balschi JA.** Hypoxia and AMP independently regulate AMP-activated protein kinase activity in the heart. *Am J Physiol Heart Circ Physiol* 288: H2412–H2421, 2005.
19. **Gustafson LA, Zuurbier CJ, Bassett JE, Barends JP, Van Beek JH, Bassingthwaighte JB, Kroll K.** Increased hypoxic stress decreases AMP hydrolysis in rabbit heart. *Cardiovasc Res* 44: 333–343, 1999.
20. **Headrick JP, Emerson CS, Berr SS, Berne RM, Matherne GP.** Interstitial adenosine and cellular metabolism during beta-adrenergic stimulation of the in situ rabbit heart. *Cardiovasc Res* 31: 699–710, 1996.
21. **Headrick JP, Peart J, Hack B, Flood A, Matherne GP.** Functional properties and responses to ischaemia-reperfusion in Langendorff perfused mouse heart. *Exp Physiol* 86: 703–716, 2001.
22. **Hoerter JA, Lauer C, Vassort G, Guéron M.** Sustained function of normoxic hearts depleted in ATP and phosphocreatine: a ^{31}P-NMR study. *Am J Physiol Cell Physiol* 255: C192–C201, 1988.
23. **Joubert F, Mazet JL, Mateo P, Hoerter JA.** ^{31}P NMR detection of subcellular creatine kinase fluxes in the perfused rat heart. Contractility modifies energy transfer pathways. *J Biol Chem* 277: 18469–18476, 2002.
24. **Kolocassides KG, Galinanes M, Hearse DJ.** Dichotomy of ischemic preconditioning: improved postischemic contractile function despite intensification of ischemic contracture. *Circulation* 93: 1725–1733, 1996.
25. **Kolocassides KG, Seymour AML, Galinanes M, Hearse DJ.** Paradoxical effect of ischemic preconditioning on ischemic contracture? NMR studies of energy metabolism and intracellular pH in the rat heart. *J Mol Cell Cardiol* 28: 1045–1057, 1996.
26. **Korvald C, Elvenes OP, Myrmel T.** Myocardial substrate metabolism influences left ventricular energetics in vivo. *Am J Physiol Heart Circ Physiol* 278: H1345–H1351, 2000.
27. **Kovacic S, Soltys CL, Barr AJ, Shiojima I, Walsh K, Dyck JR.** Akt activity negatively regulates phosphorylation of AMP-activated protein kinase in the heart. *J Biol Chem* 278: 39422–39427, 2003.
28. **Kroll K, Kinzie DJ, Gustafson LA.** Open-system kinetics of myocardial phosphoenergetics during coronary underperfusion. *Am J Physiol Heart Circ Physiol* 272: H2563–H2576, 1997.
29. **Kudo N, Barr AJ, Barr RL, Desai S, Lopaschuk GD.** High rates of fatty acid oxidation during reperfusion of ischemic hearts are associated with a decrease in malonyl-CoA levels due to an increase in 5′-AMP-activated protein kinase inhibition of acetyl-CoA carboxylase. *J Biol Chem* 270: 17513–17520, 1995.
30. **Kudo N, Gillespie JG, Kung L, Witters LA, Schulz R, Clanachan AS, Lopaschuk GD.** Characterization of 5′AMP-activated protein kinase activity in the heart and its role in inhibiting acetyl-CoA carboxylase during reperfusion following ischemia. *Biophys Biochim Acta* 1301: 67–75, 1996.
31. **Lawson JWR, Veech RL.** Effects of pH and free Mg^{2+} on the K_{eq} of the creatine kinase reaction and other phosphate hydrolyses and phosphate transfer reactions. *J Biol Chem* 254: 6528–6537, 1979.
32. **Leon H, Atkinson LL, Sawicka J, Strynadka K, Lopaschuk GD, Schulz R.** Pyruvate prevents cardiac dysfunction and AMP-activated protein kinase activation by hydrogen peroxide in isolated rat hearts. *Can J Physiol Pharmacol* 82: 409–416, 2004.
33. **Lloyd SG, Wang P, Zeng H, Chatham JC.** The impact of low-flow ischemia on substrate oxidation and glycolysis in the isolated perfused rat heart. *Am J Physiol Heart Circ Physiol* 287: H351–H362, 2004.
34. **Mallet RT, Sun J.** Mitochondrial metabolism of pyruvate is required for its enhancement of cardiac function and energetics. *Cardiovasc Res* 42: 149–161, 1999.
35. **Momken I, Lechene P, Koulmann N, Fortin D, Mateo Doan BT P, Hoerter JA, Bigard X, Veksler V, Ventura-Clapier R.** Impaired voluntary running capacity of creatine kinase-deficient mice. *J Physiol* 565: 951–964, 2005.
36. **Neely JR, Grotyohann LW.** Role of glycolytic products in damage to ischemic myocardium. Dissociation of adenosine triphosphate levels and recovery of function of reperfused ischemic hearts. *Circ Res* 55: 816–824, 1984.
37. **Ponticos M, Lu QL, Morgan JE, Hardie DG, Partridge TA, Carling D.** Dual regulation of the AMP-activated protein kinase provides a novel mechanism for the control of creatine kinase in skeletal muscle. *EMBO J* 17: 1688–1699, 1998.
38. **Pucar D, Bast P, Gumina R, Lim L, Drahl C, Juranic N, Macura S, Janssen E, Wieringa B, Terzic A, Dzeja PP.** Adenylate kinase AK1 knockout heart: energetics and functional performance under ischemia-reperfusion. *Am J Physiol Heart Circ Physiol* 283: H776–H782, 2002.
39. **Russell RR III, Li J, Coven DL, Pypaert M, Zechner C, Palmeri M, Giordano FJ, Mu J, Birnbaum MJ, Young LH.** AMP-activated protein kinase mediates ischemic glucose uptake and prevents postischemic cardiac dysfunction, apoptosis, and injury. *J Clin Invest* 114: 495–503, 2004.
40. **Sambandam N, Lopaschuk GD.** AMP-activated protein kinase (AMPK) control of fatty acid and glucose metabolism in the ischemic heart. *Prog Lipid Res* 42: 238–256, 2003.
41. **Sanders MJ, Grondin PO, Hegarty BD, Snowden MA, Carling D.** Investigating the mechanism for AMP activation of the AMP-activated protein kinase cascade. *Biochem J* 403: 139–148, 2007.
42. **Schwartz K, Boheler KR, Delabastie D, Lompre AM, Mercadier JJ.** Switches in cardiac muscle gene expression as a result of pressure and volume overload. *Am J Physiol Regul Integr Comp Physiol* 262: R364–R369, 1992.
43. **Skladanowski AC, Newby AC.** Partial purification and properties of an AMP-specific soluble 5′-nucleotidase from pigeon heart. *Biochem J* 268: 117–122, 1990.
44. **Soboll S, Bunger R.** Compartmentation of adenine nucleotides in the isolated working guinea pig heart stimulated by noradrenaline. *Hoppe Seylers Z Physiol Chem* 36: 125–132, 1981.
45. **Stein SC, Woods A, Jones NA, Davison MD, Carling D.** The regulation of AMP-activated protein kinase by phosphorylation. *Biochem J* 345: 437–443, 2000.
46. **Stepanov V, Mateo P, Gillet B, Beloeil JC, Lechene P, Hoerter JA.** Kinetics of creatine kinase in an experimental model of low phosphocreatine and ATP in the normoxic heart. *Am J Physiol Cell Physiol* 273: C1397–C1408, 1997.
47. **Ventura-Clapier R, Vassort G.** Role of myofibrillar creatine kinase in the relaxation of rigor tension in skinned cardiac muscle. *Pflügers Arch* 404: 157–161, 1985.
48. **Ventura-Clapier R, Veksler V.** Myocardial ischemic contracture. Metabolites affect rigor tension development and stiffness. *Circ Res* 74: 920–929, 1994.
49. **Ventura-Clapier R, Veksler V, Hoerter JA.** Myofibrillar creatine kinase and cardiac contraction. *Mol Cell Biochem* 133: 125–144, 1994.
50. **Viollet B, Andreelli F, Jorgensen SB, Perrin C, Geloen A, Flamez D, Mu J, Lenzner C, Baud O, Bennoun M, Gomas E, Nicolas G, Wojtaszewski JF, Kahn A, Carling D, Schuit FC, Birnbaum MJ, Richter EA, Burcelin R, Vaulont S.** The AMP-activated protein kinase α_2 catalytic subunit controls whole-body insulin sensitivity. *J Clin Invest* 111: 91–98, 2003.
51. **Xing Y, Musi N, Fujii N, Zou L, Luptak I, Hirshman MF, Goodyear LJ, Tian R.** Glucose metabolism and energy homeostasis in mouse hearts overexpressing dominant negative α_2 subunit of AMP-activated protein kinase. *J Biol Chem* 278: 28372–28377, 2003.
52. **Young LH, Li J, Baron SJ, Russell RR.** AMP-activated protein kinase: a key stress signaling pathway in the heart. *Trends Cardiovasc Med* 15: 110–8, 2005.
53. **Zarrinpashneh E, Carjaval K, Beauloye C, Ginion A, Mateo P, Pouleur AC, Horman S, Vaulont S, Hoerter JA, Viollet B, Hue L, Vanoverschelde JL, Bertrand L.** Role of the α_2-isoform of AMP-activated protein kinase in the metabolic response of the heart to no-flow ischemia. *Am J Physiol Heart Circ Physiol* 291: H2875–H2883, 2006.

Downloaded from journals.physiology.org/journal/ajpheart at Univ Catholique Louvain Bruxe (130.104.166.176) on August 18, 2020.